energies

MDPI

Article

A Power Grid Partitioning Method for Short-Circuit Current Considering Multi-Scenario Security with an Improved Direct Current Model

Wentao Zhang [1,*], Ruipeng Guo [1], Yishan Shi [1], Yuchen Tang [2] and Yi Lin [2]

[1] College of Electrical Engineering, Zhejiang University, Hangzhou 310027, China; eegrp@zju.edu.cn (R.G.); sys981103@163.com (Y.S.)
[2] State Grid Fujian Economic Research Institute, Fuzhou 350011, China; h0980164@163.com (Y.T.); liny-02@163.com (Y.L.)
* Correspondence: 848937866@163.com

Abstract: In order to ensure the security of power grids and control the level of short-circuit currents, a multi-objective optimization method for power grid partitioning is proposed. This method takes into consideration both short-circuit currents and multi-scenario safety constraints. A power grid partitioning optimization model is established to achieve objectives such as minimizing disconnected lines, maximizing safety margins, and ensuring load balance in the main transformers. The model aims to satisfy constraints related to short-circuit current levels, base-case power flow, and $N-1$ security. To address the significant deviation in the static security constraint model caused by large amounts of active power losses in large-scale power grids, an improved direct current model is proposed to reduce these errors and meet the accuracy requirements for grid partitioning optimization. Additionally, to adapt to the variability of renewable energy output, an optimization method is proposed, combining three scenarios of renewable energy generation while satisfying short-circuit current and static security constraints. The power grid partitioning model is mathematically formulated as a large-scale mixed-integer linear programming problem, which presents challenges in terms of hardware requirements and computational complexity when solved directly. To mitigate these challenges, equivalent WARD values are assigned to the short-circuit current constraints, base-case constraints, and anticipated fault-induced power flow constraints. Anticipated faults and bottleneck branches are accurately incorporated, and the problem is decomposed into smaller-scale mixed-integer linear programming problems, solved in a stepwise iterative manner. This approach significantly improves computational efficiency and meets the requirements of practical large-scale power grid applications. To validate the proposed model and algorithm, a simulation program is developed using C++, and a simulation analysis of a regional transmission network is conducted. The program ensures the correctness of the proposed model and demonstrates the effectiveness of the algorithm.

Keywords: short-circuit current; improved direct current model; multi-scenario; partition; safety constraints

check for updates

Citation: Zhang, W.; Guo, R.; Shi, Y.; Tang, Y.; Lin, Y. A Power Grid Partitioning Method for Short-Circuit Current Considering Multi-Scenario Security with an Improved Direct Current Model. *Energies* **2023**, *16*, 7332. https://doi.org/10.3390/en16217332

Academic Editors: Wei Gan, Cheng Liu, Shiwei Xia, Ying Xu and Meng Song

Received: 22 September 2023
Revised: 21 October 2023
Accepted: 25 October 2023
Published: 29 October 2023

1. Introduction

With the sustained development of the economy, the capacity and the number of substations is constantly increasing [1]. This leads to an increase in the level of short-circuit current in the grid. The rise in short-circuit current levels causes a great increase in the degree of short-circuit fault hazards, and it will seriously threaten the safe operation of equipment and grids. A short-circuit current on a bus exceeding its switch-blocking capacity is vetoed in grids' planning and operation. At present, there is a bottleneck in the technology for the improvement of breakers during the opening short-circuit current's capacity. And it is costly to further improve breakers' shading capacity. Limiting the level

of short-circuit currents and avoiding short-circuit current overruns have become important issues to be considered in operation-mode arrangements. Meanwhile, the integration of wind power into grids on a large scale, as a form of renewable energy, poses significant challenges to the safety and stability of the grids in question. This is primarily due to the inherent uncertainty associated with wind power generation. Consequently, it becomes imperative to explore suitable approaches for partitioning and limiting short-circuit currents under various multi-scenario conditions.

Currently, the main measures to limit short-circuit currents are as follows: using high-impedance transformers, installing series reactors, line disconnection, bus segmentation, and so on [1–3]. Grid partitioning is, currently, a commonly used measure to limit short-circuit currents. It mainly changes the structure and operation mode of a power grid by means of a line disconnection and a busbar segmentation operation. In [4–6], optimal transmission switching (OTS) was proposed as a partitioning method for reducing short-circuit currents. Developing a more reasonable grid partitioning method for limiting short-circuit currents is one of the main problems of grid planning [7,8].

Aiming grid partitioning adjustment methods at the goal of short-circuit currents' limitation, scholars have carried out a series of studies. The current methods mainly include the topology method, the heuristic rule method, the sensitivity analysis method, the hidden enumeration method, and the mathematical optimization method, as discussed below.

i. Topology method: The literature [9] proposes a topology searching method based on a connectivity judgment algorithm, which gives the heuristic rules of a partitioned line opening. The topology adjustment method has a better suppression effect for short-circuit currents, and its impact on a system's reliability is relatively small. The literature [10] describes limiting measures for short-circuit currents that involve dynamically adjusting the system effectively, reducing the risk of short-circuits and affecting a system's transient power-angle stability. When implementing the aforementioned measures, a specific simulation analysis should be conducted for the practical system in question.
ii. Heuristic rule method: The literature [11] denotes an algorithmic method for partitioning power networks. This method involves the detection of buses with a high potential for obtaining the desired partitioning outcome for the power network at hand. Experimental results on a benchmark dataset and a real-world provincial power grid demonstrate the algorithm's capability to uncover the inherent zonal structure within power networks. Additionally, the algorithm outperforms existing methods in its autonomous determining of the optimal number of partitions.
iii. Sensitivity Analysis Method: According to the literature [12], a sensitivity analysis-based approach is employed when searching for optimal combinations of 500 kV open-line configurations, aiming to mitigate short-circuit currents. Moreover, in the literature [13], practical transmission topology control policies are introduced. These policies leverage readily available sensitivity information from an economic generation dispatch to effectively determine the candidate lines for status changes, while ensuring the continual connectivity of the overall system.
iv. Hidden enumeration method: The literature [14] proved that there is a monotonic relationship between a bus's short-circuit current and line removal, and it proposes a full-program searching method for limiting the short-circuit current in question. It is, essentially, a hidden enumeration method, but the program optimization workload is large.
v. The literature [5] proposes a transmission-line optimization disconnection model, considering short-circuit currents and $N - 1$ security constraints, by linearizing the short-circuit current calculation model. It describes self-impedance as a linear function of whether the line is disconnected or not, and it adopts the DC (direct current) method of the trend model. The literature [6] proposes a nonlinear mixed-integer planning model for the optimal-disconnection problem, considering short-circuit current constraints, and solves it using the Bender decomposition method. The

literature [15] proposes a linear mixed-integer optimization model for the optimization of grid current-limiting operation modes. And it uses WARD equivalence to reduce the computational scale of the optimization problem, which has a good potential for practical applications.

The partitioning optimization problem needs to consider the static security of the grid. Due to the large size of the contingencies of power systems, and also due to the difficulty in solving large-scale nonlinear mixed-integer optimization problems, the DC method is generally used in grid partitioning optimization. However, the DC model concentrates the deviation of active loss in the balancing machine, and when applied to a large-scale power system, the static security constraint model accuracy cannot meet the requirements because the total amount of active loss is larger than the capacity of the generators or the circuits. This shortcoming leads to a large deviation of the currents near the balancing machine or interprovincial liaison line. The literature [16] compares the optimization results of the DC (Direct Current) method and AC (Approximate Corrective) method for the transmission line optimization disconnection problem, and it is found that the disconnection scheme given by the DC method may not be the optimal scheme, and sometimes it is not even a feasible solution. Meanwhile, as the scale of renewable energy sources such as wind turbines and photovoltaic increases in the grid, the impact of uncertainty of renewable energy output needs to be considered [16]. In this paper, we consider the renewable energy output in multiple scenarios, and jointly optimize the short-circuit partitioning method to meet multiple scenarios.

Based on the optimization model of current-limiting operation given in the literature [15], this paper proposes a multi-objective grid partitioning optimization method considering short-circuit current and static security constraints. It focuses on the problem of excessive computational volume and low accuracy of the DC method model encountered. The main work includes:

(1) Aiming at the error problem of the static security constraint model of the DC method caused by large active losses, this paper proposes a method to reduce the error of the DC method, which meets the accuracy requirements of grid partitioning optimization.
(2) Aiming at the problem that short-circuit current limiting partitioning cannot meet the requirements due to the fluctuation of renewable energy under extreme conditions, a short-circuit current partitioning method is proposed to jointly optimize multiple scenarios.
(3) Based on the multiple scenarios of grid partitioning optimization, a multi-objective optimization model is proposed to improve the reasonableness of the optimization results.
(4) Aiming at the problem of a large calculation scale of grid partition optimization, the optimization solving speed is improved by step-by-step cyclic solving, WARD equivalence, and precise addition of contingencies and monitoring branches to meet the requirements of large power systems.

2. Power Grid Short-Circuit Current Limitation Partitioning Model Considering WARD Equivalent

To address the issue of excessive error in active power near the balancing machine bus and the uncertainty of renewable energy output, which in turn prevents the DC method providing a satisfactory solution to the short-circuit current limiting problem in extreme cases, this paper divides the grid partitioning optimization method into two parts: (1) After conducting a DC method of short-circuit current limiting partitioning, the respective branch circuit's long-term load current is used as the standard deviation for measurement, along with injection of each zero-injection bus, establishing the constraints of the equation and constructing the state estimation model for the DC method. (2) Based on the improved DC method of short-circuit current partitioning, the issue of fault current partitioning in extreme situations is taken into accountment. A short-circuit current limiting partitioning

scheme is proposed by jointly optimizing the integration of different renewable energy generation scenarios, and the diagram of this method is shown in Figure 1.

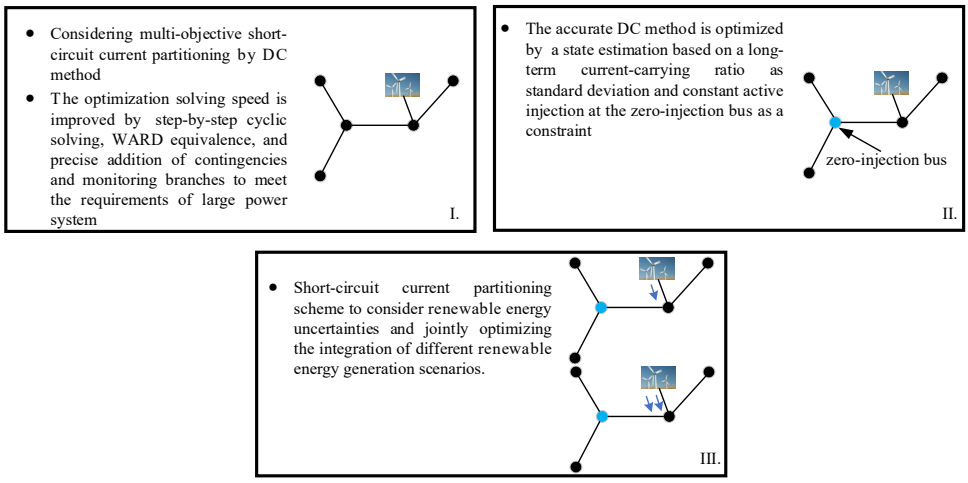

Figure 1. The diagram of power grid partition method. It denotes a diagram of the short-circuit current limiting partitioning method in 3 steps. Step I includes preprocessing the model using the WARD equivalence methodology. Step II includes using an improved DC model to overcome the disadvantage of ignoring active power loss errors in the DC model. Step III considers the optimization method under different renewable energy processing scenarios based on the modified DC model.

2.1. Power Grid Short-Circuit Current Limitation Partitioning Model

Power system partitioning aims to decrease the level of short-circuit current at the fault location in order to mitigate safety hazards caused by excessive short-circuit current when circuit breakers open. When conducting grid partitioning, it is necessary to take into accountment the following factors, which are related to short-circuit currents and security constraints [17,18].

2.1.1. Minimum Number of Weighted Open Lines

Typically, the disconnection of lines or segmentation of buses results in the loss of network frame integrity, diminishing power supply reliability and transient stability levels of the system. Therefore, grid partition optimization aims to minimize the number of weighted disconnected lines.

$$\min \sum_{ij \in S_C} W_{ij}^{O} O_{ij} \tag{1}$$

where the symbol ij denotes the line with bus numbers as its endpoints. The open state of line ij is denoted by O_{ij}, where 1 denotes a disconnected line and 0 denotes a running line. The weight of line ij being disconnected is denoted by W_{ij}^{O}, which corresponds to the penalization cost. The set of candidate open branches is denoted by S_C.

It should be noted that the term "line disconnection" here is used in a broad sense, including both the disconnection of 500 kV lines and the segmentation of 220 kV busbars.

2.1.2. Maximum Safety Margin for Currents in the Base State

The grid security margin is strongly correlated with the line loading rate. In this context, the maximum margin of security is defined as the minimum value among the maximum loading rates of each branch, represented by the following:

$$\min \alpha^{\max} \tag{2}$$

$$\alpha^{\max} \geq \frac{P_{ij}}{P_{ij}^{\max}}, \ \forall ij \in S_C \tag{3}$$

$$\alpha^{\max} \geq -\frac{P_{ij}}{P_{ij}^{\max}}, \ \forall ij \in S_C \tag{4}$$

where the variable $\alpha^{\max}$ denotes the maximum load rate among all the load rates of branches. The variables P_{ij} and $P_{ij}^{\max}$ denote the steady-state active current and long-term allowable load capacity of the branch 'ij'.

2.1.3. Load Rate Equalization for Higher-Level Main Transformers

It is crucial to ensure load balance among the higher-level (500 kV) main transformers during the operation of the sub-level (220 kV) power grid to prevent issues like decreased efficiency and increased losses. To achieve the goal of load balancing for the main transformers, a variable α^{ref} is introduced to represent the reference load rate of the main transformers.

$$\min \sum_{ij \in S_T} \left| \frac{P_{ij}}{P_{ij}^{\max}} - \alpha^{ref} \right| \tag{5}$$

2.1.4. Anticipated Fault State Power Flow Safety Objectives

The power grid must be capable of withstanding anticipated fault impacts, ensuring that the power flow of all equipment does not exceed their short-term load carrying capacity. This enables operators to effectively handle accidents. The optimization objective is to minimize the cumulative rate of anticipated fault state power flow exceeding the predefined limits.

$$\min \sum_{v \in S_v} \beta_{ij}^{(v)} \tag{6}$$

$$-\left(1 + \beta_{ij}^{(v)}\right) \overline{P}_{ij}^{\max} \leq P_{ij}^{(v)} \leq \left(1 + \beta_{ij}^{(v)}\right) \overline{P}_{ij}^{\max} \tag{7}$$

$$\beta_{ij}^{(v)} \geq 0 \tag{8}$$

where the superscript v denotes the anticipated fault number. S_v denotes the set of anticipated faults. $\beta_{ij}^{(v)}$ denotes the exceedance ratio of branch ij under the anticipated fault v. $\overline{P}_{ij}^{\max}$ denotes the short-term permissible current flow of branch ij, which is typically higher than the long-term permissible current flow $P_{ij}^{\max}$.

2.1.5. WARD Equivalent

(1) The WARD equivalent process

In Section 2.1.1, after the set of candidate open branches is established in the model, there is a substantial amount of redundant calculations of the power grid after fine-tuning the fault-free mode. Therefore, in order to reduce the size of the model, this paper uses the WARD equivalent method to perform equivalence on the power grid structure and anticipated disconnection under each anticipated fault before mathematical modeling.

For actual power grids, because the sites with excessively high levels of short-circuit currents are often concentrated in a few specific regions, the WARD equivalent method can be used to reduce the number of variables and constraints in the DC model.

Figure 2 depicts the network changes before and after WARD equivalence in a two-area interconnected system. The internal network denotes the region of interest for power grid analysis, while the external network denotes the region to be equivalenced. The two areas are connected through a boundary bus, $B_i \ldots B_j$ for the inner area and $B_m \ldots B_n$ for the outer area. After the process of WARD equivalence, the impact of the external network on the internal network is reflected through the injection of an equivalent current (or equivalent injection of active power) at the boundary bus, as well as the equivalent branches between the boundary bus and the equivalent branches to ground. The removal of the external network bus reveals the network changes before and after equivalence through variations

in branch parameters and the injection of current (or equivalent injection of active power) at the boundary bus.

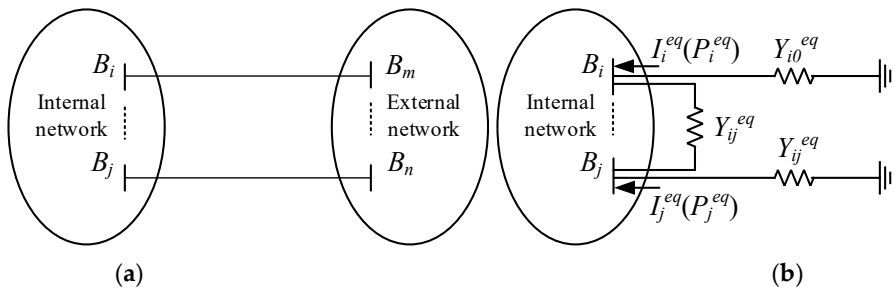

Figure 2. WARD equivalence diagram of power system. (**a**) Two-area interconnected network; (**b**) Network after WARD equivalence of the outer area.

The initial block admittance matrix for the internal bus is denoted as $Y_{II}^{(0)}$, the external bus is denoted as $Y_{EE}^{(0)}$, and the admittance matrix between internal and external bus is denoted as $Y_{IE}^{(0)}$. By adopting a bus numbering sequence that begins with the external bus and is followed by the internal bus. The system of equations to be analyzed using WARD equivalent method is as follows:

$$\begin{bmatrix} Y_{EE}^{(0)} & Y_{EI}^{(0)} \\ Y_{IE}^{(0)} & Y_{II}^{(0)} \end{bmatrix} \begin{bmatrix} V_E \\ V_I \end{bmatrix} = \begin{bmatrix} I_E^{(0)} \\ I_I^{(0)} \end{bmatrix} \tag{9}$$

Eliminate the external bus and utilize the parameters and variables of the internal bus to represent the voltage variables of the external bus, as follows:

$$V_E = Y_{EE}^{(0)-1}(I_E^{(0)} - Y_{EI}^{(0)}) \tag{10}$$

Through this transformation, the system of linear equations after WARD equivalent processing can be obtained as follows:

$$Y_{II}V_I = I_I \tag{11}$$

where $Y_{II} = Y_{II}^{(0)} - Y_{IE}^{(0)}Y_{EE}^{(0)-1}Y_{EI}^{(0)}$, $I_I = I_I^{(0)} - Y_{IE}^{(0)-1}I_E^{(0)} = I_I^{(0)} + I_I^{eq}$. These represent the equivalent admittance matrix of the bus and the injected current vector. In this short-circuit current limiting partitioning method, the V_E amplitude corresponding to the bus on both sides of the branch can be interrupted. The coefficient structure of matrix $\begin{bmatrix} Y_{EE}^{(0)} & Y_{EI}^{(0)} \\ Y_{IE}^{(0)} & Y_{II}^{(0)} \end{bmatrix}$ is used to optimize the bus numbering of part $Y_{EE}^{(0)}$, in order to maintain good sparsity and reduce the computational workload.

For the power constraints in the DC model, the WARD equivalent handling is as follows:

$$\begin{bmatrix} B_{EE}^{(0)} & B_{EI}^{(0)} \\ B_{IE}^{(0)} & B_{II}^{(0)} \end{bmatrix} \begin{bmatrix} \theta_E \\ \theta_I \end{bmatrix} = \begin{bmatrix} P_E^{(0)} \\ P_I^{(0)} \end{bmatrix} \tag{12}$$

where B denotes the corresponding admittance matrix, θ denotes phase angle vector, P denotes the inject vector of bus power. After the WARD equivalent, the system of equations is as follows:

$$B_{II}\theta_I = P_I \tag{13}$$

where $B_{II} = B_{II}^{(0)} - B_{IE}^{(0)}B_{EE}^{(0)-1}B_{EI}^{(0)}$, $P_I = P_I^{(0)} - B_{IE}^{(0)}B_{EE}^{(0)-1}B_{EI}^{(0)} = P_I^{(0)} + P_I^{eq}$. They, respectively, denote the equivalent bus admittance matrix and the injected active power vector after equivalence, and $B_{II}^{(0)}$, $B_{IE}^{(0)}$ and $B_{EE}^{(0)-1}$, respectively, denote the corresponding block

admittance matrix before equivalence. $P_I^{(0)}$ denotes the injected active power of the internal nodes before equivalence.

(2) The application of WARD in short-circuit current limiting partitioning.

The WARD equivalent processing is used to decrease the size of the optimization model for short-circuit current limiting partitioning. This process is mainly divided into two steps: determining the range of network equivalence and deriving the parameters of network equivalence. The process is as follows:

i. Determine the set of branch fault interruptions and obtain their corresponding influence zone according to the method described in the literature [15].
ii. Based on the anticipated fault set generated by step i, the influence range of the anticipated tripping is determined. The reserved network includes the anticipated tripping device and its influence range.
iii. Combine the original reserved network with the anticipated disconnection reserved network as the equivalent power grid for optimization modeling, assuming that no excessive occurrences will happen in the rest of the power grid under the anticipated disconnection.
iv. Perform WARD equivalence on the remaining part of the grid and obtain the parameters of the equivalent grid based on Equations (9)–(12).
v. According to the methods described in Section 2.2, add safety constraints.
vi. Return to step i and continue iterating through the set of valid anticipated faults until the iteration is complete.

2.2. Safety Constraints during Short-Circuit Faults

2.2.1. Safety Constraints during Short-Circuit Faults

The safety constraints during short-circuit faults include two components: the short-circuit current limit constraints for the short-circuit bus and non-short-circuit bus. For any overloaded bus f in the set of buses with excessive short-circuit currents, additional short-circuit current constraints can be added.

$$\min \sum_{f \in N_F} I_s^{(f)} \tag{14}$$

$$\sum_{g \in S_G^{(f)}} \frac{E_g''}{x_g''} + \sum_{fj \notin S_C} \frac{V_j^{(f)}}{x_{fj}} - \sum_{fj \in S_C} I_{fj}^{(f)} \leq I_{\max}^{(f)} + I_s^{(f)} \tag{15}$$

$$I_s^{(f)} \geq 0 \tag{16}$$

$$M(O_{ij} - 1) \leq I_{ij}^{(f)} \leq M(1 - O_{ij}),\ \forall ij \in S_C \tag{17}$$

$$-MO_{ij} \leq I_{ij}^{(f)} - \left(\frac{V_i^{(f)} - V_j^{(f)}}{x_{ij}} \right) \leq MO_{ij},\ \forall ij \in S_C \tag{18}$$

$$\sum_{g \in S_G^{(i)}} \frac{E_g'' - V_i^{(f)}}{x_g''} = \sum_{ij \notin S_C} \left(\frac{V_i^{(f)} - V_j^{(f)}}{x_{ij}} \right) + \sum_{ij \in S_C} I_{ij}^{(f)}, \forall i \neq f, i \in N_A \tag{19}$$

$$V_f^{(f)} = 0 \tag{20}$$

where i, j, and f all denote bus numbers. $S_G^{(i)}$ denotes the set of generators for bus i; g denotes the generator number. E_g'' and x_g'' denote the sub-transient voltage and sub-transient reactance of generator g, respectively. $V_i^{(f)}$ denotes the voltage magnitude of bus i when bus f is short-circuited. x_{ij} denotes the series reactance of branch (i, j). $I_{ij}^{(f)}$ denotes the

current flowing from bus i to bus j on branch ij when bus f is short-circuited. I_{fmax} denotes the short-circuit current limit of bus f. I_{sf} is a relaxation variable that denotes the excess of short-circuit current for bus f. When it is 0, it indicates that the short-circuit current is not excessive. When it is a positive value, it indicates that the short-circuit current level is excessive. By penalizing the excess in the objective function, the aim is to avoid excessive short-circuit currents as much as possible. This is mainly used to prevent optimization problems that may arise from the failure to meet the short-circuit current level constraints of certain overloaded buses in a single optimization. M denotes a sufficiently large positive number. N_A denotes the set of all buses.

2.2.2. Steady-State Power Flow Constraints

In the operation of the power grid, it is required that all equipment is not overloaded under normal conditions.

(3) Power balance constraints.

$$P_{Gi} - P_{Li} - \sum_{j \in S_{Bi}} P_{ij} = 0,\ \forall i \in N_A \tag{21}$$

where P_{Gi} and P_{Li}, respectively, denote the active power output of the unit and the steady-state power flow of bus i. S_{Bi} denotes the set of branches adjacent to bus i.

(4) Constraints on the flow of an openable branch.

$$\left(O_{ij} - 1\right)M \le P_{ij} \le \left(1 - O_{ij}\right)M,\ \forall ij \in S_C \tag{22}$$

$$-O_{ij}M \le P_{ij} - \frac{\theta_i - \theta_j}{x_{ij}} \le O_{ij}M,\ \forall ij \in S_C \tag{23}$$

(5) Constraints on the flow of a non-openable branch.

$$P_{ij} = \frac{\theta_i - \theta_j}{x_{ij}},\ \forall ij \in (S_B - S_C) \tag{24}$$

where θ_i denotes the phase angle of bus i under steady-state power flow, and S_B denotes the set of all branches.

2.2.3. N − 1 Anticipated Fault State Power Flow Constraints

Similar to the current constraints in steady-state, the current constraints of each N − 1 predicted fault state can be established as follows:

(1) Power balance constraints.

$$P_{Gi}^{(v)} - P_{Li}^{(v)} - \sum_{j \in S_{Bi}} P_{ij}^{(v)} = 0,\ \forall i \in N_A \tag{25}$$

(2) Constraints on the flow of an openable branch.

$$\left(O_{ij} - 1\right)M \le P_{ij}^{(v)} \le \left(1 - O_{ij}\right)M,\ \forall ij \in S_C \cap ij \notin E_v \tag{26}$$

$$-O_{ij}M \le P_{ij}^{(v)} - \frac{\theta_i^{(v)} - \theta_j^{(v)}}{x_{ij}} \le O_{ij}M,\ \forall ij \in S_C \cap ij \notin E_v \tag{27}$$

where E_v denotes the set of all branches in the N − 1 predicted fault state.

(3) Constraints on the flow of a non-openable branch.

$$P_{ij}^{(v)} = \frac{\theta_i^{(v)} - \theta_j^{(v)}}{x_{ij}}, \ \forall ij \in (S_B - S_C - E_v) \tag{28}$$

Equations (6)–(8) and (25)–(28) together constitute the N − 1 safety objective constraint. The main purpose of using objective constraints, rather than rigid constraints, is to avoid infeasibility.

3. An Improved DC Method of Short-Circuit Current Partitioning

The DC constrained model is adopted in Section 2.2, which describes the power grid partition optimization problem as a linear mixed-integer programming problem, greatly improving the efficiency and reliability of the optimization problem solution. If the AC model is used instead, the optimization problem becomes a nonlinear mixed-integer programming problem, which significantly increases the difficulty, computational complexity, and convergence reliability of the solution. And the AC model cannot meet the practical requirements of the power grid application, because the DC model ignores the active power loss. For small-scale power grids, the total amount of active power loss caused by neglecting the active power-loss-induced branch flow error is small, which can meet the engineering application requirements. However, when the DC model is applied to large-scale power systems, the total amount of active power loss in the network is large, far exceeding the capacity of a single generator or the current-carrying capacity of a single branch. Moreover, the active power loss deviation of the two flow models is entirely borne by the balancing machine, leading to significant flow deviations near the balancing machine or interprovincial transmission lines, making it difficult to meet the practical requirements of the power grid application.

To mitigate the negative impacts of inaccuracies in the DC model on the optimization model of power grid partitioning. The DC method state estimation model is constructed by taking the active current value of each branch sender as the active measurement value of the branch, taking the same proportion of the long-term current-carrying capacity of each branch (e.g., 1%) as the standard deviation of the measurement, and taking the unchanged active injection of each zero-injector bus as the constraint of the equation, as follows:

$$\begin{cases} \widetilde{P}_{ij} = \frac{\theta_i - \theta_j}{x_{ij}} + \Delta P_{ij} \ \forall (i,j) \in S_B \\ \sum\limits_{j \in N_i} \frac{\theta_i - \theta_j}{x_{ij}} = 0 \ \forall i \in S_z \end{cases} \tag{29}$$

$$PDF(\Delta P_{ij}) = \frac{1}{\sigma_{ij}\sqrt{2\pi}} e^{-\frac{\Delta P_{ij}^2}{2\sigma_{ij}^2}} \tag{30}$$

$$\sigma_{ij} = 0.01 P_{ij}^{\max} \tag{31}$$

where i and j denote the bus numbers. S_B denotes the collection of branch lines, while S_Z signifies the set of zero injection buses. N_i denotes the set of neighboring branches for bus i. P_{ij} denotes the measured active power flow from bus i to bus j through the (i, j) branch, obtained from AC calculation. ΔP_{ij} denotes the measurement error corresponding to the difference between DC and AC. $PDF(\Delta P_{ij})$ signifies the probability density function of ΔP_{ij}. σ_{ij} denotes the standard deviation for ΔP_{ij} [19].

The measurement equation for state estimation method in the power system is generally expressed as:

$$\begin{cases} z = h(x) + r \\ g(x) = 0 \end{cases} \tag{32}$$

where x denotes an n-dimensional vector of state variables; z denotes an m-dimensional vector of measured variables; $h(x)$ denotes the measurement function; r denotes the vector of measurement errors; $g(x)$ denotes an l-dimensional vector of function variables.

When both $h(x)$ and $g(x)$ are quadratic function vectors, Equation (32) is referred to as the quadratic-constrained quadratic estimation problem.

For the convenience of illustration, the equations can be denoted as

$$f(x) = \begin{bmatrix} h(x) \\ g(x) \end{bmatrix}$$

In mathematics, a quadratic function can be described as follows:

$$f_i(x) = x^T A_i x + b_i^T x + c_i \tag{33}$$

where i denotes the number of the equation. A_i denotes the n-by-n-dimensional upper triangular constant matrix. b_i denotes an n-dimensional constant vector. c denotes a constant.

Weighted least squares method (WLS) is the most widely used state estimation method in the power system. It can eliminate the interference of random Gaussian errors and achieve unbiased estimation of true values [20–22].

WLS method can be denoted in Equation (34).

$$\begin{cases} \min \quad J(r) \quad = \sum\limits_{i=1}^{m} \left(\frac{r_i}{\sigma_i}\right)^2 \\ s.t. \quad r = z - h(x) \\ \qquad\quad g(x) = 0 \end{cases} \tag{34}$$

where σ_i denotes the standard deviation of the i-th measurement.

In power systems, the measurement function $h(x)$ is a nonlinear function. Therefore, when solving the WLS model, it is necessary to linearize the function $h(x)$. We can expand the function around $x = c$ using Taylor series and retain the linear term.

$$h(x) \approx h(x_0) + H(x_0)\Delta x \tag{35}$$

where $\Delta x = x - x_0$, $H(x)$ denotes the m-by-m-dimensional measurement Jacobian matrix.

$$H(x_0) = \left.\frac{\partial h(x_0)}{\partial x}\right|_{x=x_0} \tag{36}$$

In the traditional Newton's method for solving equations, Equation (34) is commonly handled as a high-precision measurement at point a. In this case, a new measurement function can be defined by converting Equation (34).

$$\begin{cases} \min \quad J(r) \quad = \sum\limits_{i=1}^{m} \left(\frac{r_i}{\sigma_i}\right)^2 \\ s.t. \quad r = z - h'(x) \end{cases} \tag{37}$$

By substituting Equation (35) into Equation (37) and solving, the following iterative equation is obtained.

$$\begin{cases} \Delta x = [H'^T(x_{k-1}) W H'(x_{k-1})]^{-1} H'^T(x_{k-1}) W r_{k-1} \\ x_k = x_{k-1} + \Delta x_k \end{cases} \tag{38}$$

where $H''(x)$ is the Jacobian matrix of the new matrix '$h'(x)$', W denotes the diagonal weight matrix, and $W_{ij} = 1/\sigma_i$.

By performing iterative calculations on Equation (38), the results of state estimation can be obtained. If the objective function and constraint conditions in model (34) are polynomial functions up to the second degree, the state estimation problem described by Equation (34) can be formulated as a quadratic constraint estimation model. This enables the decoupling of modeling and algorithm solving, allowing for the direct use of the primal-

dual interior point method to solve Equation (34). When the measurement function is quadratic in this model, the generation of the Jacobian matrix is greatly facilitated. The formation of modified equations when using the primal-dual interior point method for solving is also convenient. This significantly enhances the computational efficiency and convergence.

The steps for the improved DC method are denoted in Equations (39) and (40). In order to decrease the deviation of active power loss generated by the line, this study applies an estimation denoted in Equations (29)–(31).

$$\min J(\boldsymbol{\theta}) = \sum_{(i,j)\in S_B} \left(\frac{\widetilde{P}_{ij} - \frac{\theta_i - \theta_j}{x_{ij}}}{\sigma_{ij}} \right)^2 \tag{39}$$

$$s.t. \sum_{j\in N_i} \frac{\theta_i - \theta_j}{x_{ij}} = 0 \; \forall i \in S_Z \tag{40}$$

The solution to the quadratic programming problem involving Equations (39) and (40) enables the determination of the phase angles for each bus in the system. Consequently, it facilitates the adjustment of the active power output of the generators and the active power of the load.

The proposed correction method possesses two key characteristics.

i. Firstly, it yields reduced discrepancies in branch loadings when compared to the initial AC calculation results by utilizing the modified DC calculation. By utilizing the modified DC, it becomes possible to model the power flow constraints for steady-state and anticipated fault conditions. This modeling approach offers improved computational accuracy to meet the demands of large-scale practical power system applications.
ii. Secondly, this method solely rectifies the active power values of existing loads and power sources while refraining from introducing virtual power sources or loads to zero injection bus. Hence, it preserves the integrity of the original network structure and minimizes the impact on the algorithmic procedures.

4. The Method for the Short-Circuit Current Limitation Partitioning Problem in the Power Grid

The problem of short-circuit current limitation programming is mathematically a linear mixed-integer optimization problem, which can be solved using commercial optimization software such as CPLEX. For large-scale power grids, the expected scale of fault sets is enormous, describing all safety constraints directly in the optimization problem would result in an extremely large computational scale, posing significant challenges for numerical solutions. In the literature [15], the effective fault set is determined using fault impact domains, and only the effective fault set is modeled to reduce the scale of the optimization problem using the WARD equivalent reduction. In practical applications, the method based on the WARD equivalent value can achieve better results.

In long-term power grid planning, as power source distribution and grid structure change significantly, it is essential to reevaluate the optimal partitioning scheme. Specifically, for a future power grid in operation, the measures for partitioning and resolving loops need reconsideration.

In such cases, the grid has multiple buses with excessive short-circuit currents, significant exceedances, and a high number of candidate lines for opening. Solving large-scale linear mixed-integer optimization problems still poses challenges due to computational complexity. In the context of linear mixed-integer optimization problems, the number of integer variables is the key factor that affects the computational speed of algorithms. Solving multiple small-scale optimization problems is much faster than solving a single large-scale problem. This paper, therefore, uses an iterative approach. In each iteration,

only the candidate lines for opening are selected and optimized for the buses with the most severe exceedances. The process continues until all nodes with excessive short-circuit currents are resolved. The optimization process initially omits considering the N − 1 security constraints. Subsequently, safety constraints related to predicted faults and exceedance lines violating the limits are gradually incorporated. The iteration repeats until no new predicted fault-induced exceedance lines emerge. Figure 3 illustrates the flowchart of the algorithm, which consists of the following steps [23–25]:

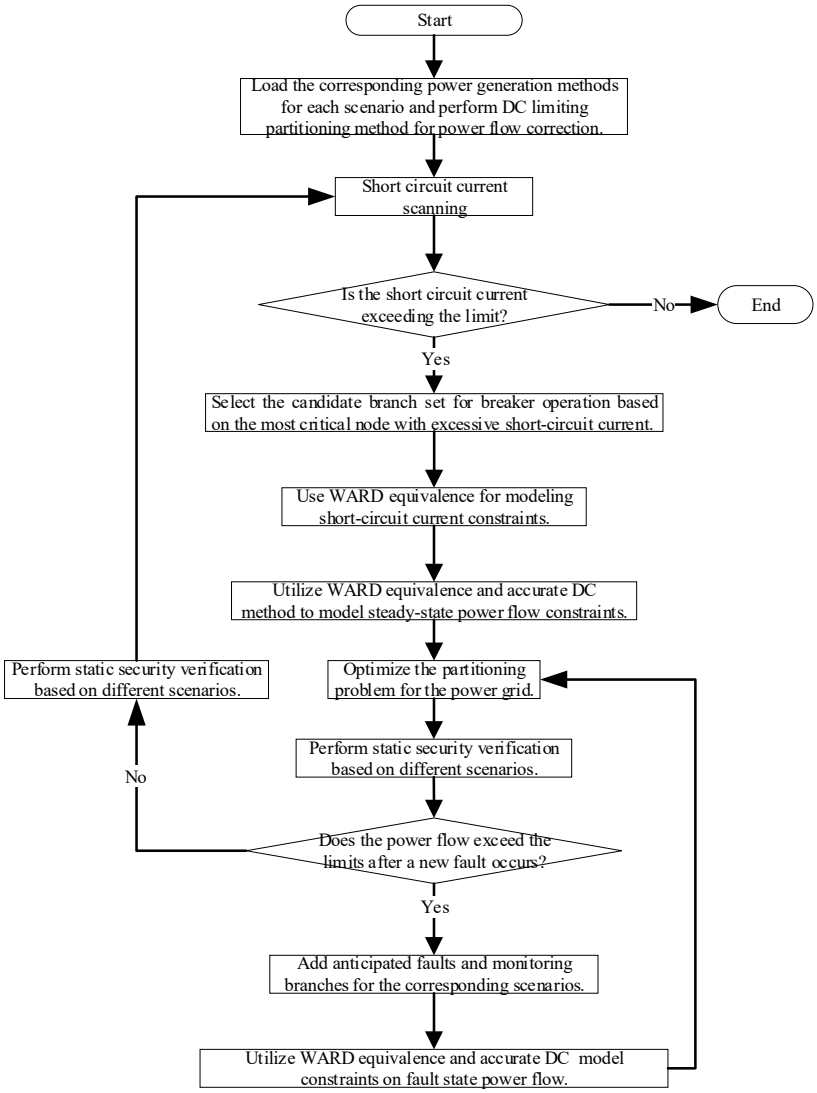

Figure 3. The flow chart of power grid partition method.

i. Initialize and modify the improved DC state for each scenario based on the method described in Section 3.
ii. Determine the bus with excessive short-circuit currents through short-circuit current scanning, and select the bus with the most severe excess for optimization. If there are no nodes with excessive short-circuit currents, the optimization is finished.
iii. For buses with excessive short-circuit currents, select a candidate set of branch closures based on the short-circuit current branch coefficient and whether the network constraints are satisfied after the closure, in order to reduce the optimization size.
iv. Apply the WARD equivalent method to model the short-circuit current constraints, keeping only the adjacent node set of the short-circuit current exceedance points and the candidate branch closures.

v. Select the steady-state power flow monitoring branch set based on the influence range of the candidate branch closures.
vi. Model the steady-state power flow for each scenario using the WARD equivalent method and DC, keeping only the candidate branch closures, the steady-state monitoring branches, and their adjacent nodes to reduce the size of the optimization problem.
vii. Add static safety constraints for each scenario and perform optimization calculations.
    (a) Solve the optimization problem of power grid partitioning.
    (b) Use the improved DC method to perform static security verification for each scenario.
    (c) If all scenarios meet the static safety constraints, proceed to step ii; otherwise, for each scenario and anticipated fault, add the most severe branch with flow exceeding limits into the monitored branch set.
    (d) Use the WARD equivalent and improved DC method to model the anticipated fault state flow for each scenario, keeping only the candidate disconnected branches, fault monitoring branches, and their adjacent bus to minimize the size of the optimization problem. Proceed to step (a).

During iterations from Step ii to Step vii, which is aiming to eliminate all issues of excessive short-circuit currents at the buses [26,27].

5. Example Analysis

Based on the partition optimization model and solution method proposed in this article, a simulation program was developed using C++. The simulation analysis was conducted on a certain region's power transmission network. The simulation environment consisted of a laptop with an Intel(R) Core (TM) i5-12400F CPU and 16 GB of memory. The optimization solver used was CPLEX.

The optimization model proposed in this article is analyzed for a specific region in East China. In this case study, approximately 6.5 million kilowatts of centralized wind power and 2 million kilowatts of centralized solar power, among other renewable energy sources, are connected to multiple nodes in the region.

5.1. Analysis of Results from the Improved DC Method

For this system, the power flow results are calculated using the DC method, improved DC method, and AC method. Table 1 presents the deviation of the load rate. The load factor rate of each line is computed, and the 11 lines with the highest load factor rate deviations under the improved DC method are selected. The results are denoted in Table 2.

As can be seen in Table 1, the improved DC method reduces the average deviation from 0.32% to 0.26% and the maximum deviation from 95.23% to 7.13%.

By referring to Table 1 and Equation (41), the load factor rate deviations can be compared between the DC and the improved DC methods relative to the AC method.

$$Deviation(\%) = |FactorRate_{DCPF} - FatorRate_{ACPF}| \tag{41}$$

Selecting the 11 lines with the highest load rates, the load factor deviation under the DC method and improved DC methods are as follows in Figure 4.

Table 1. Load factor rate deviation for DC method and improved DC method.

DC Method		Improved DC Method	
Maximum Deviation (%)	**Average Deviation (%)**	**Maximum Deviation (%)**	**Average Deviation (%)**
95.23	0.32	7.13	0.26

Table 2. Load factor rate under three types of power flow calculation methods.

Line	DC Method Power (MW)	DC Method Load Factor Rate (%)	Improved DC Method Power (MW)	Improved DC Method Load Factor Rate (%)	AC Method Load Factor Rate (%)
Mpt-Myc	−143.8	9.7	−221.3	14.9	7.8
Mdt-Mlz	3.7	0.6	−26.9	5.0	10.1
Mlz-Mtt	0.3	0.1	−31.7	10.0	14.7
Mjm-Msx	−34.9	1.2	−88.4	3.3	7.1
Mcs-Mmq	3.8	1.1	55.3	15.3	19.1
Mbz-Mqy	−5.3	1.5	29.5	8.1	11.8
Mdt-Mgs	10.7	2.4	−3.3	0.8	4.0
Msk-Myc	−133.3	9.0	−110.3	7.4	5.8
Mmq-Msk	4.3	0.6	56.4	7.8	10.7
Msy-Msk	197.2	10.9	581.4	32.3	29.5
Myd-Myx	73.3	2.6	525.5	19.0	16.2

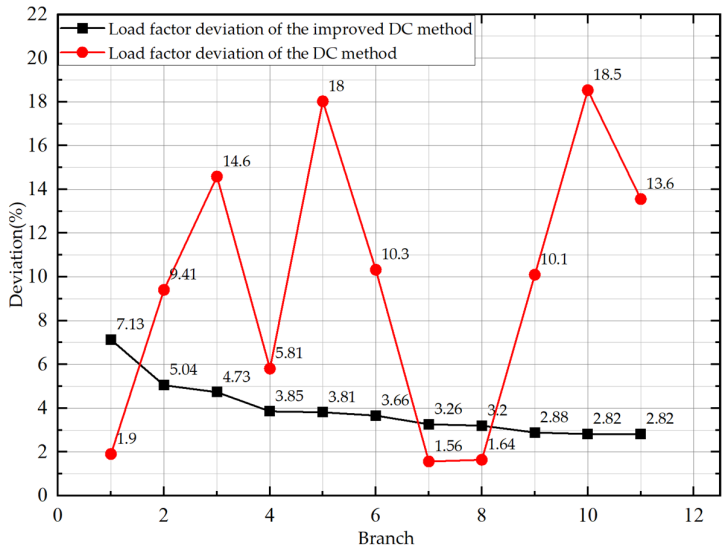

Figure 4. Change in branch load factor after using the improved DC method.

Select the 11 lines with the highest deviation rate in this area, and compare the load deviation of the lines using the DC method and the improved DC method. It is evident that the deviation rate is significantly lower for lines 2, 3, 5, 6, 9, 10, and 11 when using the improved DC method. For lines 1, 4, 7, and 8, the deviation rates are slightly higher using the improved DC method, but the difference is not significant. It can be observed that the improved DC method results in lower deviations, better fulfilling the accuracy requirements of the power grid.

5.2. The Example Analysis of Joint Optimization Considering Multiple Scenarios

In actual power grids, the most severe faults at the same bus are generally three-phase short-circuits or single-phase ground faults. Therefore, these two types of short-circuit faults are considered here.

In the simulation, the partitioning optimization of a 220 kV power grid in Eastern China was carried out. This region includes 10 openable lines, 4 units of 500 kV main transformers, three 500 kV substations and six 220 kV substations. The red lines represent the 500 kV substations and their operational transmission lines, the black lines represent the 220 kV substations or operational transmission lines, the green lines represent the 500 kV

main transformers, the yellow lines represent the openable lines in the model, and the yellow dashed lines represent the planned openable lines in the model.

In order to adapt to the transmission demands of the summer operational mode of the power grid and the power export demands of new energy development, this paper proposes a network planning optimization decision-making scheme that satisfies both static security constraints and short-circuit current limitations. This optimization method jointly optimizes three different scenarios of new energy output. Four operational scenarios are considered as input:

i. High demand during summer.
ii. High wind power generation during peak wind periods.
iii. High wind power and solar power generation during peak wind periods.
iv. Joint optimization of scenario i, scenario ii, and scenario iii.

Table 3 denotes the comparison of short-circuit currents before and after grid partition. In this paper, the short-circuit currents limitation of the buses is set to 50 kA. According to Table 3, before partitioning the number of buses with excessive short-circuit current is 28. After partitioning, the short-circuit currents of all buses do not exceed the allowable value of 50 kA.

Table 3. The comparison of short-circuit currents before and after grid partition.

Number	Bus Name	Short-Circuit Current before Partitioning/(kA)		Short-Circuit Current after Partitioning/(kA)	
		Three-Phase Short-Circuit	Single-Phase Short-Circuit	Three-Phase Short-Circuit	Single-Phase Short-Circuit
1	Mcs21	51	40.55	40.65	30.05
2	Mmh23	67.13	58.63	45.43	29.85
3	Mmh21	67.09	58.62	33.82	32.58
4	Mzm21	52.16	40.09	31.3	26.42
5	Mdt21	83.49	75.77	34.94	31.1
6	Mgq21	60.77	51.52	41.8	29.33
7	Mjx21	58	49.1	33.56	25.35
8	Mfw21	56.89	47.58	32.37	24.93
9	Mgs21	51.4	42.44	22.07	19.16
10	Mfz21	51.97	46.44	43.69	40.1
11	Myz21	58.9	48.22	31.4	27.7
12	Mcp21	54.26	43.89	26.73	23.16
13	Mnj21	51.76	42.18	22.38	19.32
14	Mxn21	54.55	45	31.66	24.97
15	Mjm21	68.94	61.53	49.67	44.37
16	Mjt21	61.34	53.39	46.72	41.6
17	Mdt22	83.52	75.79	48.55	41.56
18	Mlz21	63.77	55.58	40.34	34.36
19	Mwd21	53.91	49.02	37.65	34.03
20	Myd22	63.68	70.28	39.83	39.32
21	Mks21	63.01	55.88	48.18	43.49
22	Mxf21	52.52	44.38	38.53	33.19
23	Mdf21	51.63	42.89	37.73	31.53
24	Myd21	63.69	70.29	45.69	49.69
25	Msj21	59.94	63.45	44.78	47.47
26	Mtt21	51.14	43.15	31.45	26.4
27	Mjm22	68.88	61.47	39.04	27.45
28	Myz22	58.88	48.19	30.22	14.6

If all 28 buses with excessive short-circuit currents are directly selected as candidate branches for optimization during grid partitioning, and if they are modeled, the computational complexity of the optimization problem will be extremely large, making it currently difficult to solve. Using the short-circuit current partitioning method described in this paper.

After a total of five rounds of optimization, the calculation times for joint optimization from scenario i to scenario iii are presented in Table 4 with a value of 135.3 s. The calculation time meets the operational demands of the actual power grid.

Table 4. Calculation time for four scenarios.

Scenario	i	ii	iii	iv
Calculation time (second)	69.6	104.5	56.7	135.3

Based on the improved DC model, The grid partitioning results for combined scenarios i, ii, and iii are shown in Figure 5.

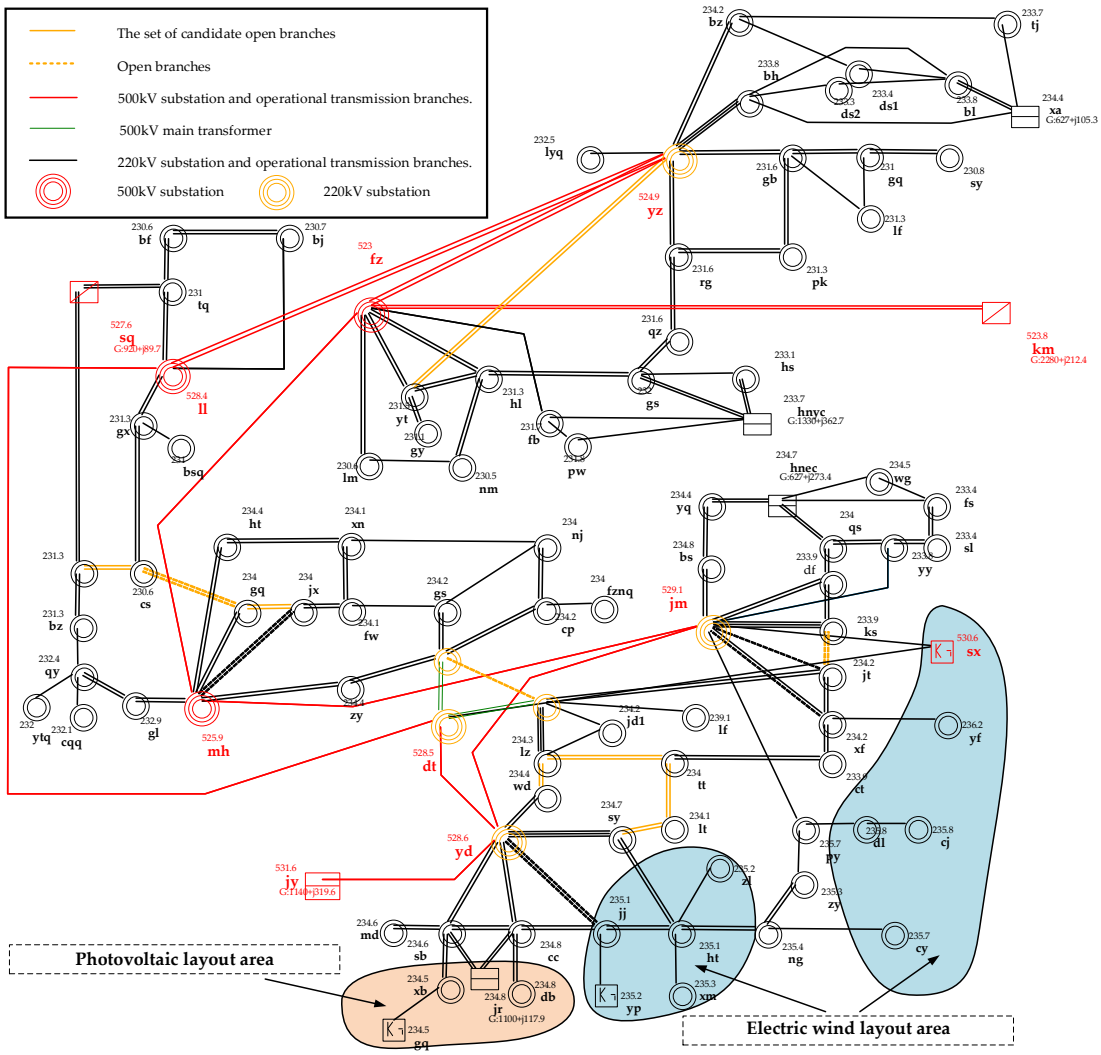

Figure 5. The optimized partition result of the real power grid.

i. The set of candidate branches that can be opened are denoted in yellow line.
ii. The result of the open branches is denoted by the yellow dotted line.
iii. The 500 kV substation and operational transmission branches are denoted by the red line.
iv. The 500 kV main transformers are denoted by the green line.
v. The 220 kV substation and operational transmission branches are denoted by the gray line.
vi. The 500 kV substations are denoted by the red cycle.
vii. The 220 kV substations are denoted by the yellow cycle.

viii. The area where photovoltaic loaded is denoted by the yellow color.
ix. The area where electric wind loaded is denoted by the blue color.

According to the partitioning results, the area is divided into four parts. In areas where PV and electric wind loaded, the network is run unlooped by disconnecting branches to reduce short-circuit currents.

In this case study, several buses in the southeastern area of the power grid have connected approximately 6.5 million kilowatts of centralized wind power and 2 million kilowatts of centralized photovoltaic power. After optimization, five transmission lines were disconnected, and the power grid was divided into five regions. This partitioning scheme meets the requirements of static security verification, and the partitioning structure is clear and adaptable. It can be accepted by power grid planning professionals.

6. Conclusions

A power grid partitioning method for short-circuit current based on multi-scenario security with improved DC model is raised in this paper approach to mitigate short-circuit currents, enhance reliability, and improve operational efficiency within the power grid. To address the significant deviation in the static security constraint model of the improved DC method, induced by substantial active power losses in large-scale power grids, a method for reducing constraint model errors is proposed in this paper. This method aims to meet the accuracy requirements of grid partition optimization. By considering equivalent WARD values for short-circuit current, base case, and anticipated fault-induced power flow constraints, and precisely incorporating anticipated faults and bottleneck branches, this paper decomposes the partition problem into multiple smaller-scale mixed-integer linear programming problems. Each problem is solved iteratively in a stepwise manner, leading to a substantial improvement in computational speed, which satisfies the requirements for practical large-scale power grid applications.

In general, the proposed stepwise iterative solving method can achieve relatively optimal partition schemes. However, it is not capable of theoretically attaining the optimal solution to the partition problem. Achieving improved zoning schemes within acceptable timeframes for practical large-scale power grids remains an area for future research.

Author Contributions: Conceptualization, W.Z. and R.G.; methodology, W.Z.; software, R.G.; validation, W.Z., R.G. and Y.S.; formal analysis, Y.T.; investigation, W.Z. and Y.S.; writing—original draft preparation, W.Z., Y.S., Y.T. and Y.L.; writing—review and editing, W.Z. and Y.S.; supervision, R.G., Y.T. and Y.L. All authors have read and agreed to the published version of the manuscript.

Funding: This research was funded by State Grid Fujian Electric Power Co., Ltd. Technology Project, grant number [52130N210005].

Data Availability Statement: Publicly available datasets were analyzed in Section 4 of this study. These data can be found here: https://matpower.org/docs/ref/matpower7.1/menu7.1.html (accessed on 25 June 2023).

Conflicts of Interest: The authors declare no conflict of interest.

References

1. Schmitt, H. Fault current limiters report on the activities of CIGRE WG A3 16. In Proceedings of the 2006 IEEE Power Engineering Society General Meeting, Montreal, QC, Canada, 18–22 June 2006; pp. 1–5. [CrossRef]
2. Yang, D.; Zhao, K.; Liu, Y. Coordinated optimization for controlling short circuit current and multi-infeed DC interaction. *J. Mod. Power Syst. Clean Energy* **2014**, *2*, 274–284. [CrossRef]
3. Hu, Y.; Chiang, H.-D. Optimal Placement and Sizing for Fault Current Limiters: Multi-Objective Optimization Approach. In Proceedings of the 2018 IEEE Power & Energy Society General Meeting (PESGM), Portland, OR, USA, 5–10 August 2018; pp. 1–5. [CrossRef]
4. Tang, S.; Li, T.; Liu, Y.; Su, Y.; Wang, Y.; Liu, F.; Gao, S. Optimal Transmission Switching for Short-Circuit Current Limitation Based on Deep Reinforcement Learning. *Energies* **2022**, *15*, 9200. [CrossRef]
5. Yang, Z.; Zhong, H.; Xia, Q.; Kang, C. Optimal Transmission Switching with Short-Circuit Current Limitation Constraints. *IEEE Trans. Power Syst.* **2016**, *31*, 1278–1288. [CrossRef]

6. Tian, S.; Wang, X.; Zhang, Q.; Qi, S.; Dou, X. Transmission switching considering short-circuit current limitations. In Proceedings of the 2017 IEEE Conference on Energy Internet and Energy System Integration (EI2), Beijing, China, 26–28 November 2017; pp. 1–6.
7. Fisher, E.B.; O'Neill, R.P.; Ferris, M.C. Optimal transmission switching. *IEEE Trans. Power Syst.* **2008**, *23*, 1346–1355. [CrossRef]
8. Marquardt, R. Modular multilevel converter topologies with DC-short circuit current limitation. In Proceedings of the 8th International Conference on Power Electronics-ECCE Asia, Jeju, Republic of Korea, 30 May–3 June 2011; pp. 1425–1431. [CrossRef]
9. Xin, Q.; Jie, H.; Bin, H.; Qiulong, N.; Gang, X.; Jinghao, Z. Study on the influence of short-circuit current limitation measures by dynamic adjustment of topology on system reliability based on graph theory. *Power Syst. Technol.* **2023**, 1000–3673. [CrossRef]
10. Yi, H.; Weijiang, C.; Bin, H. A Study on the Influence of Short-circuit Current Suppression Measures Based on System Topology Dynamic Adjustment on System Transient Power Angle Stability. *Power Syst. Technol.* **2022**, *47*, 2069–2077. [CrossRef]
11. Lixiong, X.; Junyong, L.; Yang, L.; Jing, G.; Zhanxin, Y.; Li, Z.; Yang, W. A Load Current Field-Based Algorithm for Partitioning Power Networks. *Power Syst. Technol.* **2015**, *39*, 1039–1044. [CrossRef]
12. Dong, Y.; Qinyong, Z.; Yutian, L. Short circuit current limiting strategy optimization based on sensitivity analysis. *Electr. Power Autom. Equip.* **2015**, *35*, 111–118. [CrossRef]
13. Pablo, A.R.; Justin, M.F.; Aleksandr, R.; Michael, C.C. Tractable transmission topology control using sensitivity analysis. *IEEE Trans. Power Syst.* **2012**, *27*, 1550–1559.
14. Zhang, Z.; Ning, Z.; Hao, W.; Ying, W.; Liang, C.; Bo, Y. Method of Searching All Feasible Breaking-line Schemes for Limiting Short-circuit Current. *Proc. CSU-EPSA* **2020**, *32*, 51–56+64. [CrossRef]
15. Xiawei, L.; Wei, W.; Bo, W.; Xu, H.; Yu, H.; Wei, B. A grid operation mode optimization method for controlling short-circuit current level based on WARD equivalence. *Power Syst. Prot. Control* **2017**, *45*, 128–136. [CrossRef]
16. Alcala-Gonzalez, D.; García del Toro, E.M.; Más-López, M.I.; Pindado, S. Effect of Distributed Photovoltaic Generation on Short-Circuit Currents and Fault Detection in Distribution Networks: A Practical Case Study. *Appl. Sci.* **2021**, *11*, 405. [CrossRef]
17. Yi, L.; Yuchen, T.; Wentao, Z.; Ruipeng, G.; Wei, W. A DC Estimation Method to Improve the Accuracy of DC Power Flow. *J. Phys. Conf. Ser.* **2023**, *2474*, 012058. [CrossRef]
18. Huaichang, G.; Qinglai, G.; Hongbin, S.; Bin, W.; Boming, Z. Multivariate statistical analysis-based power-grid-partitioning method. *IET Gener. Transm. Distrib.* **2016**, *10*, 1023–1031. [CrossRef]
19. Shuqing, Z.; Yanan, Z.; Kaijian, O.; Siqi, Y.; Qi, G.; Yubo, S.; Luyuan, T. Efficiency enhancement method without grid partitioning for hard real-time transient simulation of large power grids. *IET Gener. Transm. Distrib.* **2018**, *12*, 3963–3971. [CrossRef]
20. Zhenyu, M.; Aoyu, L.; Jialu, L.; Jian, Z.; Yong, M.; Wei, L.; Sijia, T.; Ligang, Z. An Active Partitioning Method for Urban Power Grid to Deal with External Attacks in Extreme Cases. In Proceedings of the 2022 IEEE 3rd China International Youth Conference on Electrical Engineering (CIYCEE), Wuhan, China, 3–5 November 2022; pp. 1–8. [CrossRef]
21. Li, H.; Zhang, X.; Han, W.; Li, Y.; Kang, A. A power grid partitioning optimization method based on fractal theory. *Int. Trans. Electr. Energy Syst.* **2019**, *29*, e2741. [CrossRef]
22. Golshani, A.; Sun, W.; Sun, K. Advanced power system partitioning method for fast and reliable restoration: Toward a self-healing power grid. *IET Gener. Transm. Distrib.* **2018**, *12*, 42–52. [CrossRef]
23. Wang, Z.; He, J.; Xu, Y.; Crossley, P.; Zhang, D. Multi-objective optimisation method of power grid partitioning for wide-area backup protection. *IET Gener. Transm. Distrib.* **2018**, *12*, 696–703. [CrossRef]
24. Abou Hamad, I.; Israels, B.; Rikvold, P.A.; Poroseva, S.V. Spectral matrix methods for partitioning power grids: Applications to the Italian and Floridian high-voltage networks. *Phys. Procedia* **2010**, *4*, 125–129. [CrossRef]
25. Zhang, X.; Chen, Y.; Wang, Y.; Ding, R.; Zheng, Y.; Wang, Y.; Zha, X.; Cheng, X. Reactive voltage partitioning method for the power grid with comprehensive consideration of wind power fluctuation and uncertainty. *IEEE Access* **2020**, *8*, 124514–124525. [CrossRef]
26. Yang, C.; Cheng, T.; Li, S.; Gu, X.; Yang, L. A novel partitioning method for the power grid restoration considering the support of multiple LCC-HVDC systems. *Energy Rep.* **2023**, *9*, 1104–1112. [CrossRef]
27. Nasiakou, A.; Alamaniotis, M.; Tsoukalas, L.H.; Vavalis, M. Dynamic Data Driven Partitioning of Smart Grid for Improving Power Efficiency by Combinining K-Means and Fuzzy Methods. In *Handbook of Dynamic Data Driven Applications Systems*; Springer International Publishing: Cham, Switzerland, 2022; Volume 1, pp. 513–535. [CrossRef]